Working with Nematic Liquid Crystals

Studying the Birefringence, and Calculating the Splay (k_{11}) and Bend (k_{33}) Elastic Constant for 8CB Liquid Crystal Compound.

NITIN JHA

ADVISOR: PROF. (DR) PRAMODA KUMAR

ADVANCED LAB 5: EXPERIMENTAL SOFT MATTER PHYSICS / COMPLEX SYSTEMS (PHY-3050)

ASHOKA UNIVERSITY, INDIA

Abstract

Contents

Chapter 1

Introduction to Liquid Crystals

A liquid crystal is a *mesophase*[1] which is often described by the anisotropy of various properties without the existence of any *3D* crystal lattice. Liquid crystals display characteristics similar to those of fluids, such as having low viscosity and the inability to support shear, and are capable of forming and merging droplets. At the same time, they exhibit anisotropic crystalline properties in fields such as optics, electricity, and magnetism, among others.[2]

1.1 Properties of Liquid Crystals

Liquid crystals are long rod-like molecular structure , and they are more or less directed along a particular axis, and have strong dipolar attraction.[2]

1.1.1 Structure of Liquid Crystals

By definition, crystalline structures have 'long range periodic ordering in three dimensions.' A liquid crystalline structure has an intrinsic (local) tendency to align along a common axis, known as **local director**. This is contrary to the behavior of liquids where there's no fixed intrinsic order of the molecules. A schematic representation of the three phases are shown in fig(1.1),

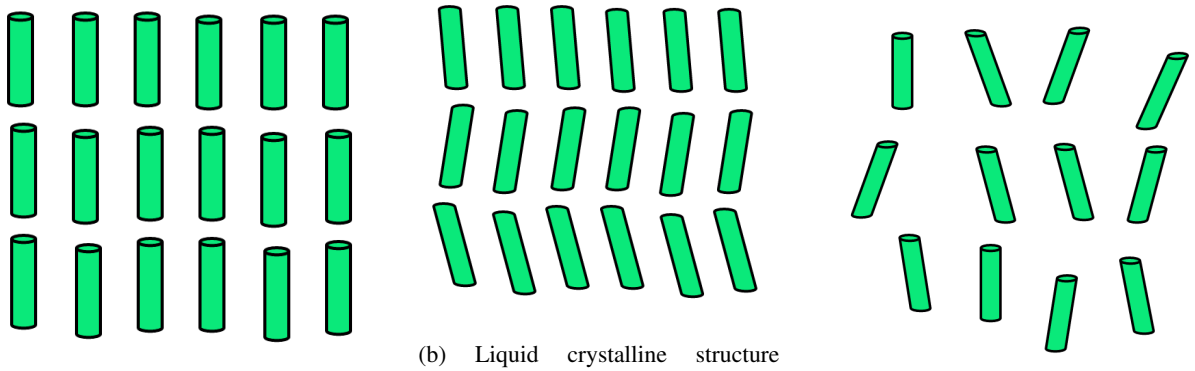

(a) Solid Crystalline Structure

(b) Liquid crystalline structure (Mesophase)

(c) Liquid Phase

Figure 1.1: Schematic of the three phases– solids, liquid-crystals, and liquid.

The presence of anisotropy in the molecular shape is a necessary, albeit insufficient, requirement for the formation of the liquid crystal phase. Liquid crystal molecules can have a diverse range of anisotropic structures, usually characterized by a central rigid core composed of two or more aromatic rings and one or more flexible alkyl chains.

[1] Phase present in the temperature range of solids and isotropic liquid phase.

[2] A dipole arises when we've two electric charges separated by a small distance.

[2] Some of the famous mesogenic shapes consists of rod-like (*calamitic*), disk-like (*discotic*), and *boomerang type structure*. All of these are displayed in the fig(1.2).

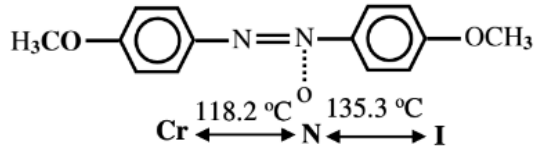

(a) *4,4-dimethyloxyazoxybenzene*. Rod-like structure of liquid crystal (Calamatic). [3]

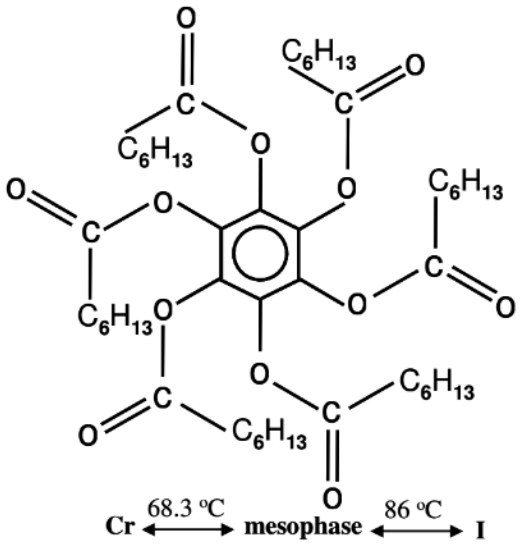

(b) *hexa-n-alkanoates of benzene.* Disc like structure (discotic) of liquid crystal. [4]

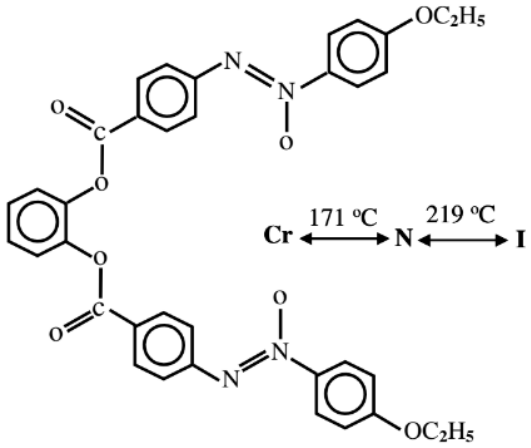

(c) *1,2-phenylene bis-[4(ethoxyphenylazoxy)benzoate].* Boomerang like structure of liquid crystal. [5]

Figure 1.2: Different possible shapes of liquid crystal components. [6]

Substances that are not as ordered as solids, but have local orientation unlike liquid phase are classified as liquid crystals.

Birefringence of Liquid Crystals

Birefringence, also known as double refraction, is a fascinating optical phenomenon that occurs when light passes through certain materials and splits into two separate rays, each with a different refractive index and velocity. When unpolarized light enters a birefringent material, it gets split into two rays that travel along different paths with different velocities. These rays are known as the *ordinary ray* and the *extraordinary ray*. The ordinary ray obeys Snell's Law and follows the standard rules of refraction, while the extraordinary ray experiences a different refractive index and deviates from the ordinary ray. As a result, birefringent materials can produce a range of optical effects, such as double images, color shifts, and polarization changes. There can be both positive and negative birefringence. The following shows fig(1.3) shows the definition of both the positive and negative

birefringence.

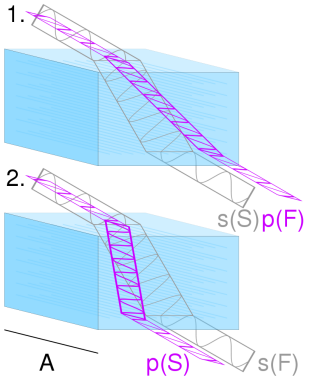

Figure 1.3: In positive birefringence (1), the ordinary ray (p-polarisation) which is perpendicular to optic axis A is faster than the extraordinary ray (S). In case of negative birefringence (2), the above is opposite, i.e., extraordinary ray is faster than the ordinary ray. [8]

Birefringence has a wide range of applications in various fields. In microscopy, it is used to analyze and identify minerals and crystals, as different crystal structures exhibit unique birefringent properties. In telecommunications, birefringent materials are used in devices such as waveplates and polarizers to manipulate the polarization state of light. Liquid crystal displays (LCDs) also rely on birefringence to control the passage of light through the liquid crystal layers to produce images.

1.2 Phases of Liquid Crystals

Thermotropic liquid crystal phases exhibit long-range orientational order in one direction and short-range correlations in other directions. In some mesophases, there may also be positional order in one or two dimensions. These liquid crystal phases can be broadly categorized into two types, *smectic* and *nematic*, depending on whether positional order is present. Overall, the presence or absence of positional order and the extent of orientational order in different directions determine the specific properties and behavior of each type of liquid crystal phase.[2] There's another phase, *cholesteric phase*, in which A helix can be described by the preferred direction of molecular orientation in successive imaginary planes. A schematic representation of all of these phases are described in fig(1.4).

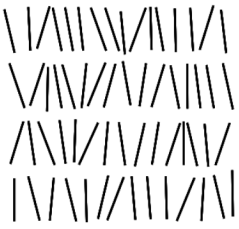

(a) *Scmetic Phase* of liquid crystals.

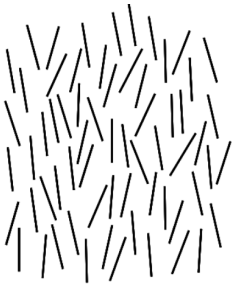

(b) *Nematic Phase* of liquid crystals.

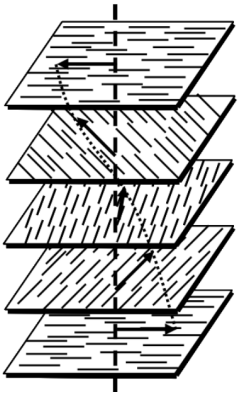

(c) *Cholestrolic Phase* of liquid crystals

Figure 1.4: Different possible phases of liquid crystal. [2]

Smectic liquid crystals consist of molecules arranged in equidistant layers with periodic molecular centers of mass in one dimension. The simplest type of smectic (Smectic A) has molecular axes oriented perpendicular to

the layers. Further classification of smectics is based on the orientation of the long axes with respect to the layer normal and the degree of positional order within the layers. In the Smectic C phase, for example, the molecules are tilted uniformly with respect to the layer normal and lack in-layer positional order. The nematic phase is a spatial fluid with long-range orientational order of the constituent molecules' long axes. A chiral nematic phase or cholesteric phase has a nematic-like local order, but a preferred orientation direction forms a helix, which may have a pitch comparable to optical wavelengths. [2] For this laboratory work, we mostly work with the liquid crystals in nematic phase.

Nematic Phase Liquid Crystals

In liquid crystals, the nematic phase is the state with the least order, where the shape-anisotropic molecules are free to move without any correlation between their centers of mass. However, the long axes of the molecules tend to align parallel to each other within thermal fluctuations. The average orientation of the long molecular axes over time and space is represented by a unit vector, $\vec{n}$, known as the *director* (discussed in the earlier section), which gives an overall indication of the nematic order. [2] The probability of finding the orientation of these molecules in nematic phase in *anti-parallel* and *parallel* orientation is equal. Thus, all the other perpendicular directions to this director $\vec{n}$ are equivalent, the medium can be classified as uniaxial. [2]

Intrinsic Deformations Present in the structure

"*Deformation*" of a crystal just refers to the variance of the director field across the given space. [7] These deformations are mainly studied under the static case mainly because the continuum equations for the dynamic nematic stage are becomes quite complicated. The structure parameter can be considered undisturbed by these deformations as long as the scale of these defects are larger than the average molecular length. [7] As expected, the crystal resists the formation of such defects as an external force must be applied to tackle the inter-molecular forces which tends to align them. To quantify the behavior of these defects, one can develop a linear elastic theory of these local directors, $\hat{n}$ (director field). The symmetry of the director field allows the presence of three **independent** kinds of deformations which is illustrated in fig(1.5). Due to these three elastic deformities, we've three types of elastic constant to quantify these defects. [7]

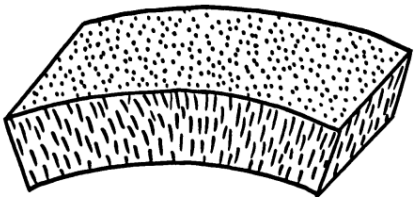

(a) *Splay*-Deformations, which corresponds to elastic constant k_{11}.

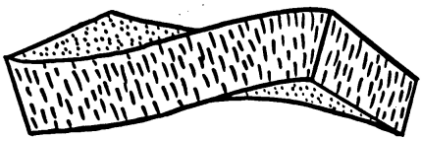

(b) *Twist*-Deformations, which corresponds to elastic constant k_{22}.

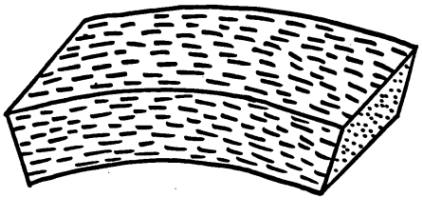

(c) *Bend*-Deformations, which corresponds to elastic constant k_{33}.

Figure 1.5: Three types of allowed deformations in the Liquid Crystals. [7]

Splay Defect occurs when the director, which is the direction of molecular alignment in a liquid crystal, rotates about an axis perpendicular to the director axis. This results in a distortion of the local ordering of molecules in the liquid crystal, forming a wedge-shaped region where the director changes direction. Splay defects can occur spontaneously due to thermal fluctuations or external disturbances, and their presence can affect the optical and electrical properties of liquid crystals. Both splay and bend defects affect the optical properties of liquid crystals, leading to changes in their *refractive index*, *birefringence*, and *polarization* behavior.

Chapter 2

Theory of the Fréedericksz Transition

Before we delve into the mathematical explanation of Fréedericksz Transition, we'll look briefly at the structural ordering of Liquid Crystals.

2.1 Structural ordering in Crystals

Crystallinity implies the presence of some sort of ordering at atomic level dimensions. The unique properties and applications of liquid crystals depend greatly on their structure and order. The alignment and orientation of liquid crystal molecules determine their anisotropic behavior, which is useful in areas such as optics and electronics. Various scientific techniques have been employed to examine the structural order of liquid crystals, including microscopy, X-ray diffraction, and spectroscopy. Researchers have used high-resolution X-ray diffraction to determine the molecular orientation in chiral liquid crystals, while polarizing microscopy has been utilized to observe defects in liquid crystal textures. These studies have provided valuable insight into the structural order of liquid crystals and their applications in modern technology. To determine the order of the molecules in a crystal, an order parameter (S) is defined. S can be used to find the order to molecules in the liquid crystals, and upon taking the average we find that at local scales they are aligned in one particular directions– also known as *local director*. The order parameter is often defined as,

$$\mathcal{S} = \frac{1}{2}\left\langle 3\cos^2\theta - 1 \right\rangle \tag{2.1}$$

In eq(2.1), θ is the angle made by the molecule to the local director as shown in fig(2.1).

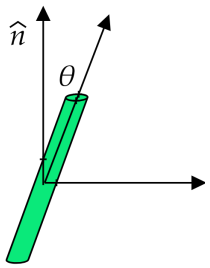

Figure 2.1: Depiction of deviation of the molecular structure from the local director direction.

For perfect crystalline structure, the order parameter is found to be one, whereas for liquid crystals the order parameter is found to in the following range, $0.3 < \mathcal{S} < 0.9$. The anisotropic nature of the liquid crystals gives rise to their unique optical properties.

2.2 Electrical Fréedericksz Transition

The Fréedericksz transition is a phenomenon that occurs in liquid crystal. It refers to the change in the alignment of liquid crystal molecules in response to an applied electric field. Liquid crystals are made up of elongated molecules that tend to align in a particular direction called the "director" when no external forces are applied.

However, when an electric field is applied to a liquid crystal, it can alter the orientation of the director, leading to the Fréedericksz transition. To understand the the transition, we'll look at the experimental schematic diagram shown in fig(2.2).

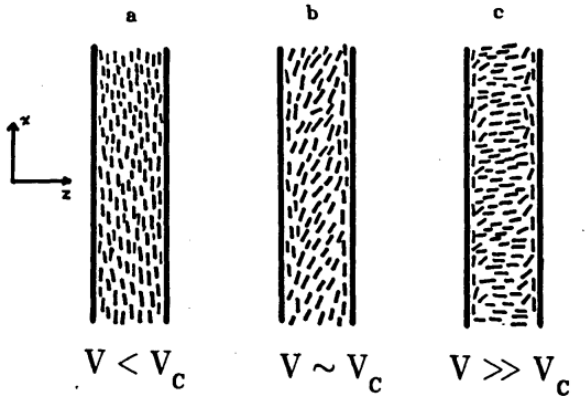

Figure 2.2: Schematic Representation of Fréedericksz Transition. [7]

Consider the above setup, first we enclose liquid-crystal sample in between the chamber of the parallel plate capacitor we made using the ITO coated cells. We assume now that the director is aligned in the x-direction. Considering the capacitors to be made by the planes defined by $z = 0$ and $z = L$, where L is the thickness of the cell. At zero voltage, the crystal should ideally be directed in x-direction. As we keep on increasing the voltage, we see that the there's not much change in the orientation of the director, but after a particular voltage (critical voltage), we see the directors starts getting deformed (fig(2.1 (b))). For values much greater than the critical voltage (v_c), we see that the director almost aligns with the externally applied electric field ($\vec{E}$). This critical voltage can be mathematically defined as,

$$V_c = \pi\sqrt{\frac{k_{11}}{\epsilon_0 \Delta\epsilon}} \tag{2.2}$$

Where, k_{11} is the splay elastic constant. We can see that for voltages lesser than the critical voltage (v_c), elastic energy is dominant. Whereas, for voltages greater than the critical voltage (v_c), the electrical energy is dominant. [7] The mathematics involved is fairly complicated, and for the sake of simplicity we'll explore the final relationships obtained between quantities of our interest wihtout doing the entirety of derivation. All the formulae have been taken from (Morris, 1986). [7] For our calculation we introduce the two "reduced" constants, [1]

$$\boxed{\gamma = \frac{\epsilon_{||}}{\epsilon_{\perp}} - 1} \tag{2.3}$$

and

$$\boxed{\kappa = \frac{k_{33}}{k_{11}} - 1} \tag{2.4}$$

Using this we can write an equation for V_c by eliminating $\Delta\epsilon$ as follows,

$$\boxed{V_c = \pi\sqrt{\frac{k_{11}}{\epsilon_0 \epsilon_{\perp} \gamma}}} \tag{2.5}$$

Now, using the above constants, we can define a reduced voltage as,

$$\boxed{v = \frac{V}{V_c} - 1} \tag{2.6}$$

[1] The boxed equation serves as a highlight to which equations were extremely important for data analysis.

2.2.1 Capacitance

Capacitance, as we know, can be descried as the amount of electric charge and the potential difference the junctions looked at. We can write capacitance for parallel plate capacitor as,

$$C = \frac{\epsilon A}{d} \tag{2.7}$$

Where, A is the area of the parallel plates, and d is the distance between the parallel plates. Now, for our experiment, we can write the Zero Voltage capacitance as,

$$C = \frac{A\epsilon_0\epsilon_\perp}{d} \tag{2.8}$$

where A: is the area of the cell used, and d is the thickness of the cell used. Now, we introduce the idea of reduced capacitance,

$$\boxed{c = \frac{C}{C_0} - 1} \tag{2.9}$$

Now, in terms of κ, γ, and reduced voltage v, we can write reduced capacitance c as,

$$c = \frac{2\gamma}{\kappa + \gamma + 1} v \tag{2.10}$$

The value of κ can be calculated from here as,

$$\boxed{\kappa = \gamma \left(\frac{2}{S_{LFC}} - 1 \right) - 1} \tag{2.11}$$

where, S_{LFC} is the slope of the linear fit between reduced voltage, v, and reduced capacitance, c at low voltage limit. using the value of κ, we find the value of k_{33} as,

$$k_{33} = (\kappa_{\text{LFC}} + 1)k_{11} \tag{2.12}$$

These are the main equations that were used for DATA ANALYSIS. The derivation of all such formulae are very complicated and thus skipped in this section. All the formulae and modifications has been taken from (Morris 1986).

2.3 Optical Fréedericksz Transition

The data analysis for the optical Fréedericksz trastion is very complicated, and is not included in this report as the final data analysis could not be done in the given time frame. We consider that the light polarized parallel to the director orientation has refraction index $n_{||}$, and the perpendicular component is $n_\perp$. The birefringence of the material can thus be written as,

$$\Delta n = n_{||} - n_\perp \tag{2.13}$$

The index $n_{||}$ is often termed as ordinary index, and $n_\perp$ as extraordinary index. [7] At zero voltage, we can write the phase difference as,

$$d_0 = \frac{2\pi L}{\lambda} \Delta n \tag{2.14}$$

Now, we can also define the reduced refraction index (ν) as,

$$\nu = \frac{n_{||}^2}{n_\perp^2} - 1 \tag{2.15}$$

Defining reduced phase, δ as,

$$\delta = 1 - \frac{d}{d_0} \tag{2.16}$$

Now, we can relate the birefringence to reduced refraction index as,

$$\frac{n_{||}}{\Delta n} = \frac{\sqrt{1+\nu}}{\sqrt{1+\nu} - 1} \tag{2.17}$$

Chapter 3

Interfacing the LCR-Meter

One important aspect to advanced experimental techniques is automating the machines which further helps in taking long term data without human intervention and thus saving a lots of time and further reducing any sorts of human error while recording the data. Automation of these machines are also known as "Interfacing" which can be done through any programming language, e.g., PYthon, MATLAB, C, etc. For this lab, the interfacing was done using PYthon.

3.1 Important Libraries

The following are the libraries used in PYthon for the Interfacing task.

```
# Important Libraries used
import numpy as np
import matplotlib.pyplot as plt
import pyvisa
import pandas as pd
```

3.2 Identifying the Device

The first step towards interfacing is connecting to the device. We need to find appropriate commands to bridge between the machine's language and python commands. This done using the SCPI commands as specified in the instruction manual of particular machine, in our case the KeySight LCR Meter.

```
# This is done using the PY-VISA Library of PYthon
rm = pv.ResourceManager("@py")
print(rm.list_resources())
```

The above command gives the address of the machine connected to the computer through which we are completing the Interfacing task.

3.3 Connecting to the Device

Now we need to connect to the device, and reset the machine before we start taking the data.

```
# Address of the device, and resetting the data
lcrmeter = rm.open_resource('USB0::10893::12033::MY46622603::0::INSTR')
lcrmeter.write("*RST")
```

Now that we've successfully connected to the device, we need to prepare the device for taking data. For this part, we find take the reading for voltage vs capacitance at two different frequencies.

3.4 Taking the Reading

We create an input arrays of the range of voltage for which we need to see the relationship between voltage and capacitance. We can extract data using *.query("FETCH?")* command.

```
#range of input voltages
voltage_input = np.arange(0.1, 10, 0.1)

#empty arrays to store the data
cap = []
voltage=[]
ou_cap = []

#defining the frequency
lcrmeter.write("FREQ 10000")

#increasing the voltage and storing the data
for i in tqdm.tqdm (voltage_input):
    time.sleep(2)
    #taking each point 32 times
    lcrmeter.write(':APER 32')
    lcrmeter.write(f":VOLT:LEVEL {i}")
    #.query("FETCH?") is used to get data from the machine
    out_cap = float(lcrmeter.query("FETCH?").split(",")[0])
    voltage.append(i)
    ou_cap.append(out_cap
```

3.5 Making .csv File

Now, we need to store the data on our device such that we can share it easily. The following is the code that was used to do the above. First, we create a dataframe and then save it on the device in a *.csv* format.

```
mytable = pd.DataFrame({ "Input Frequency " : voltage, "Output Capacitance(0.5 V)":
                                                    out_cap,})

#defining the path and name of the .csv file
mytable.to_csv("/Users/ankitgupta/Desktop/nitin_lab5_2.csv")
```

3.6 Disconnecting the Device

We've successfully connected to the device and have successfully taken the required data, we now need to disconnect from the machine. The following code shows how to disconnect from the device.

```
lcrmeter.close() #disconnecting from the device
```

In this next chapter, we go step-by-step into the experimental techniques used across the semester towards studying the optical nature of Liquid Crystal and understanding the Freedricksz Transition for the Liquid Crystals.

Chapter 4

Experimental Methodology

There were several steps taken to complete this experiment to study the Fréedericksz Transition. The following chapter will explore each step in some details.

4.1 Cell Preparation

To conduct our experiment we need to fill Liquid Crystal in a chamber created by two ITO-coated glass plates separated by a mylar-spacer such that it acts like a parallel plate capacitor. Preparing the cell itself consisted of several steps such as making pattern on the cell, cutting in appropriate sizes, gluing them with a mylar spacer, soldering over the edges, etc. This section explores various such important steps that were taken to construct our cell for measurements.

4.1.1 Cell Pattern and Etching

The glass plates are coated with Indium Tin Oxide (ITO) which makes the surface conducting. Now, we need to make a parallel plate capacitor using these plates. To do so we need to strategically by removing the ITO coating from certain areas. ITO coating can be removed using sulphuric acid (H_2SO_4), this process is known as *Etching*. To do so the following steps were taken,

1. Find the ITO coated side of the glass plate by checking for conductivity using a multi-meter.
2. Cover the area where ITO coating is needed with a plastic-tape. Make sure to double coat the area to ensure no accidental leakage of the acid and accidental removal of the conducting layer.
3. The patterned cell was now kept into a petri-dish and H_2SO_4 was poured over it. It was covered with a cone-shed to be safe from the chemical fumes. The cell was left to rest in the acid for about $30 - 40$ mins.
4. Once the cell was etched, the plastic-coating was removed from the cell. There we have our patterned cell ready for the experiment.

4.1.2 Preparing Solution and Coating

After the cell is prepared, it needs to be coated with a PVA solution of known concentration. For our case, $0.508\ g$ of PVA (polyvinyl alcohol) was mixed in $7.00\ mL$ cold water. The mixture was then shaken well using the machine 'Eppendorf Mixmate.' After the solution was made, it was kept in the refrigerator to get rid of the foam produced during the shaking process. 'EZ-Spin A1' machine was then used to coat the glass slide by putting few drops of the above solution and rotating the slide slowly and then at a higher rpm. This way the entirety of the glass slide with more or less uniform coating of the above polymer. Fig(4.1) shows of the setup of the machine used to coat the glass slide with the polymer to come a step closer to the complete the preparation of the cell.

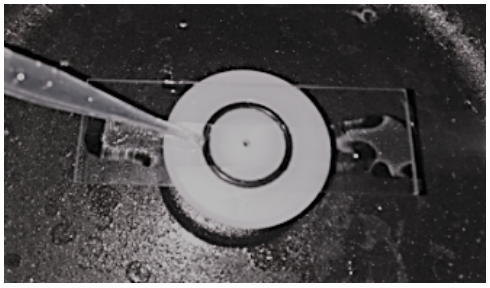

Figure 4.1: Polymer coating on the patterned and etched glass slide.

4.1.3 Baking and Rubbing of the Cell

This is the third step in the preparation of the cell to be used to study the Freedricksz transition. Once the glass slide is coated with PVA solution, it needs to be baked. This step is important because it'll reduce the chances of the polymer coating getting scratched out easily from the surface. The slide coated with the polymer is kept in 'Rotex' hot-air oven and is baked for temperatures upto $120°C$ for 90 mins. Inside the oven, the cell is also cooled down to the room temperature. Once, the cell is baked it needs to be rubbed which will align the polymer strands in on particular direction. This was done using 'HO-IAD-BTR-03' machine. Fig(4.2) shows a schematic diagram of the setup used to rub the cells.

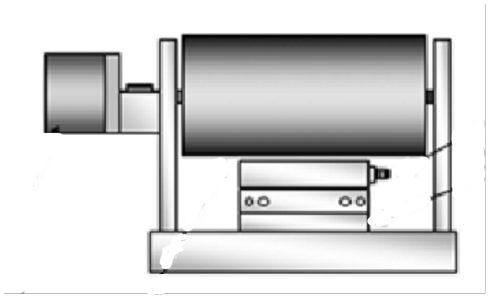

Figure 4.2: Schematic Representation of the machine used to rub the cell to align the polymers in one particular direction. [9]

4.1.4 Cutting the Slides

Cutting the glass slides to make cells is one of the important steps. It is advised to be done carefully as this is one of the last steps towards the creation of the cells. Improper cutting techniques can cause scratches in the polymer coating as thus the arrangement of the liquid crystals inside the cell at the later stage will be inconsistent. The cells were cut into half along their width using a diamond pointed cutter. The were further cut into another halves to make a total of two cells. Fig(4.3) shows an experimental picture for which shows the cutting of a normal glass slide using a diamond-pointed cutter.

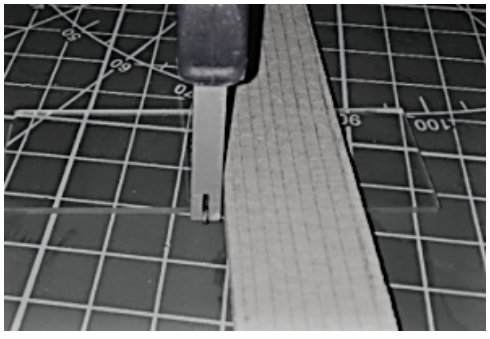

Figure 4.3: Picture which shows how a glass slide is cut in the lab using a diamond-pointed cutter.

4.1.5 Gluing the Glass Plates and Making the Chamber

Once the glass plates are cut into 4 pieces, we need to make a chamber from them. To make a chamber out of it, we need to glue two pieces together using a mylar-spacers. For the preparation of my cell, a mylar spacer of 21 microns was used. We take two cut pieces, and glue them together with the conducting ITO sides facing each other spaced using the mylar sheet. Fig(4.4) shows a schematic represenation of a glued almost finished cell.

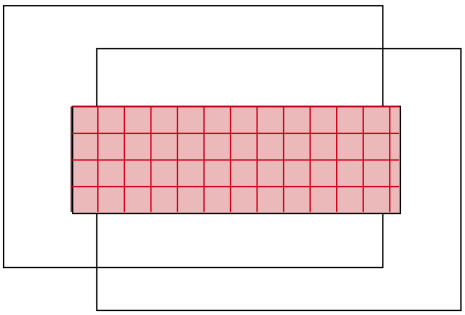

Figure 4.4: Schematic representation of two ITO coated glass slides glued together with a mylar spacers. The area shaded with the red represents the overlapping of two ITO coated cells with the conducting side facing each other. This process helps in formation of a chamber in between the ITO slides where Liquid-Crystals can be filled for studying their optical properties.

4.1.6 Completing the Cell

Now that we've made a chamber using our patterned slides, we need to solder wires onto it to make a capacitor out of it. As our experiment requires use of electric field to study the Freedricksz transition, we need some way of passing electric current through our cell. This needs us to solder wires onto our cell, but soldering directly onto glass is difficult and thus we need to do first put a small coat of Indium. The copper wires were now soldered over the indium coating. Fig(4.5) represents a completed diagram of how the final soldered cell will look like.

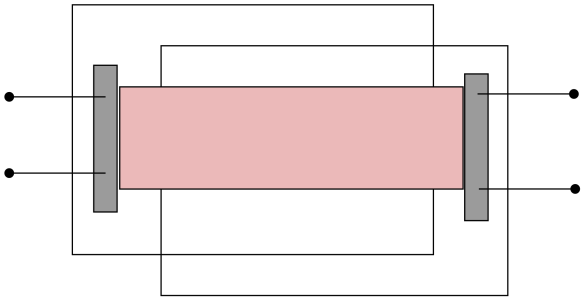

Figure 4.5: Final diagram of the cell, where the gray area represents the Indium coating where wires are soldered. The red area represents the area where the IPA coating is intact, i.e., conducting areas over the glass plates.

4.2 Experimentation using Cell

4.2.1 Filling of Liquid Crystals

Once the cell was made, we used the phenomenon of the capillary action to fill the liquid crystal in the chamber formed between the plates and mylar spacers. We used a room-temperature Liquid Crystal (5CB). We put the liquid crystal at the edge of the cell, due to the capillary action the liquid crystal seeps in and spreads uniformly throughout the cell. This ensures that there are no air bubbles present in our filled cell.

4.2.2 Focusing the Microscope

As the cell is ready for experimentation, we'll need to focus the microscope to observe the optical properties of the liquid crystal filled inside it. Since, the experiment requires temperature variations– we need the sample to be mounted on a heat stage. The cell was fixed inside the heat stage using Teflon cello-tape, due to the high melting point of Teflon. This will ensure that even at high temperature readings the cell is fixed at its particular position, and this will ensure that our readings are not affected by this. The heat stage was kept under the microscope and the microscope was focused accordingly.

4.3 Determining the Thickness of the Cell

After preparation of the cell and before filling it with liquid crystal compound– we need to find the thickness of the shell. For this we use the following two method, and compare the results in the next chapter.

4.3.1 Mach-Zehnder interferometer: "Pohl" Interferometery

The Pohl interferometer, also called the Mach-Zehnder interferometer, is an optical device used to track minute variations in a substance's refractive index. It entails splitting a light source into two beams, recombining them, and measuring the interference pattern that results. When the interferometer is used to measure changes in the refractive index of a material, one of the beams is passed through the substance while the other is not. Any variations in the two beams' refractive indices will then be visible in the ensuing interference pattern. The Pohl interferometer has many uses in optics, including determining the optical characteristics of materials and creating new optical devices. The following equation describes the working formula for Phol Interferometer,

$$d = \frac{Z\lambda(n^2 - \sin^2\theta)^{1/2}}{2\Delta x \sin\theta\cos\theta} \tag{4.1}$$

where, the following are the quantities used,

- d is the thickness of the glass-slide.
- Z is the distance between the screen and the glass slide.
- θ is the angle at which the glass-slide is rotated with respect to the laser-path.
- Δx is the distance between two fringes (either dark or light).

For our experiment, we used a modified setup which can be used to determine the thickness of the glass-slide as the path difference gets introduced due to the finite thickness of the glass slide used.

4.3.2 UV Spectroscopy

The analytical method known as UV-Vis spectroscopy measures the amount of discrete wavelengths of UV or visible light that are absorbed by or transmitted through a sample in comparison to a reference or blank sample. This property may be affected by the sample composition, which may disclose what is in the sample and at what concentration. Fig(4.6) shows a schematic diagram which shows the working of a UV-spectrometer. [10]

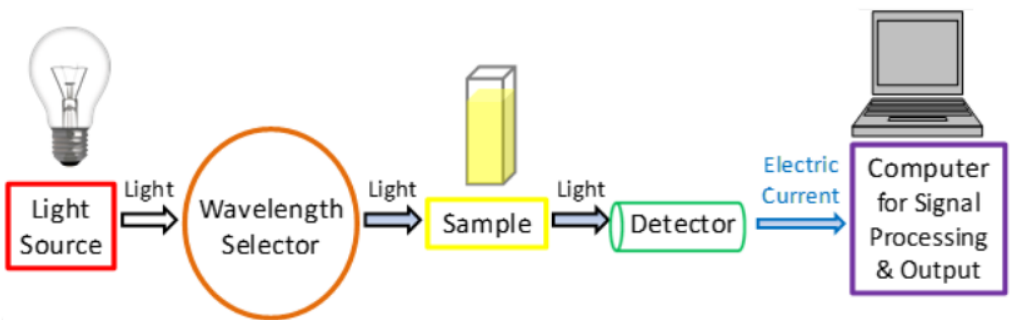

Figure 4.6: Schematic diagram which shows steps involved in UV-spectroscopy. [10]

After the light passes through the sample, a detector is used to turn it into an audible electronic signal. The base of a detector is often made of semiconductors or photoelectric coatings. Once the current is produced, the signal is passed through a computer. Fig(4.7) shows the internal setup through which the transmitted light can be used to find the thickness of the slide put into the spectrometer.

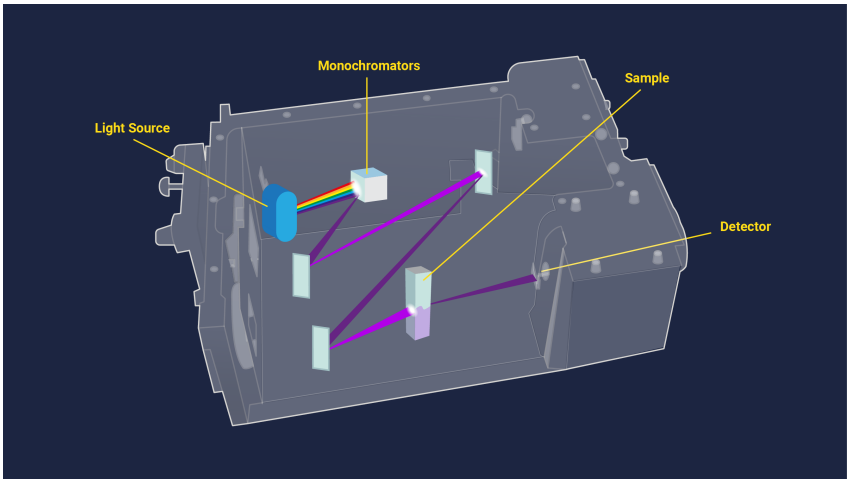

Figure 4.7: Internal working of UV-spectrometer. [10]

The formula used for this technique is given as,

$$d = \frac{n\lambda_1\lambda_2}{2(|\lambda_1 - \lambda_2|)} \tag{4.2}$$

These were the major experimental techniques used across this experiment involving Liquid-Crystals. In the next section, we'll move on to data analysis and error analysis for different sections of this experiments.

Chapter 5

Data Analysis

5.1 Interfacing Data

We use the interfacing command to get the measurement of output capacitance for input voltage for a cell containing $8CB$ sample and $5CB$ sample.

5.1.1 5CB Sample

After interfacing the LCR-Meter, we took voltage vs capacitance data for two different frequencies, i.e., $f_1 = 1kHz$ and $f_2 = 10kHz$. The following is the graph obtained for $5CB$ sample for capacitance vs frequency.

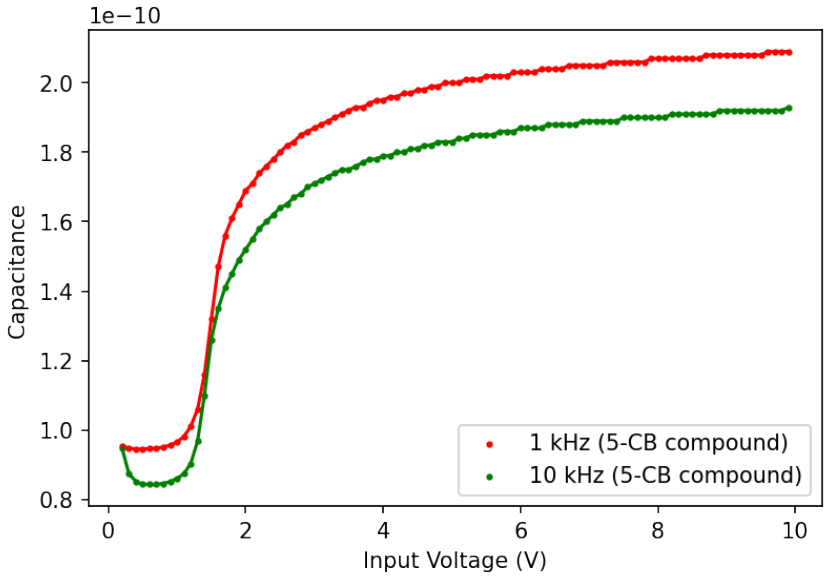

Figure 5.1: Graph obtained through interfacing code for $5CB$ Liquid Crystal compound at two different frequencies, i.e., $f_1 = 1kHz$ and $f_2 = 10kHz$.

We see that both the curves are not overlapping each other. This can be associated with the possibility of air pockets present inside the prepared cell.

5.1.2 8CB Sample

To verify our measurements, we used our code to take data for $8CB$ sample at two different frequencies, i.e., $f_1 = 5kHz$ and $f_2 = 10kHz$. The following is the graph obtained for $8CB$ sample,

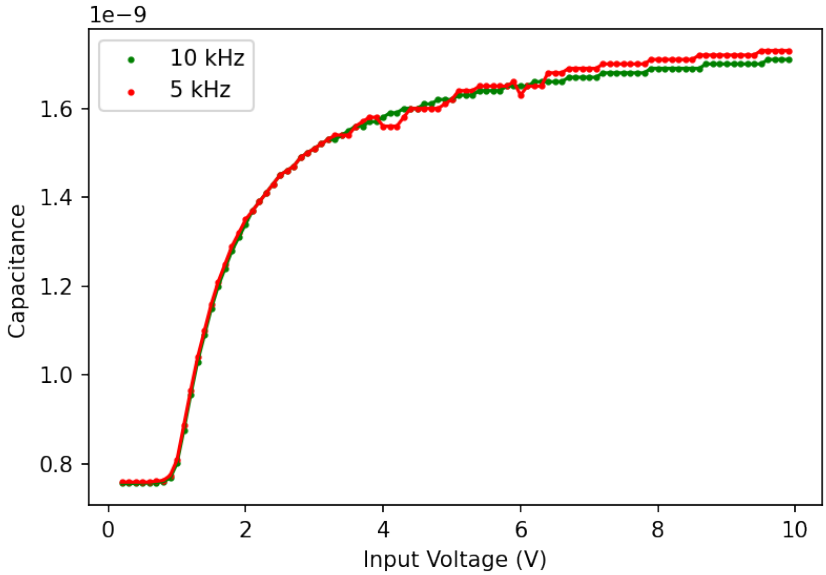

Figure 5.2: Graph obtained through interfacing code for $8CB$ Liquid Crystal compound at two different frequencies, i.e., $f_1 = 5kHz$ and $f_2 = 10kHz$.

Now, we can see that both of the graphs are overlapping each other as expected. This verifies that our interfacing code is working perfectly, and that the problem associated with the quality of cell containing $5CB$ liquid-crystal compound.

5.2 Thickness of the Cell

We measured the thickness of our prepared cell using both the UV-spectroscopy method and the Pohl-interferometry technique. First, let's look at the measurement through the UV-Spectrometer,

5.2.1 UV-Spectrometer Measurement

We put the cell in the UV-spectrometer, and get the graph between the transmittance percentage (%) vs various different wavelength. Fig(5.3) shows the graph obtained.

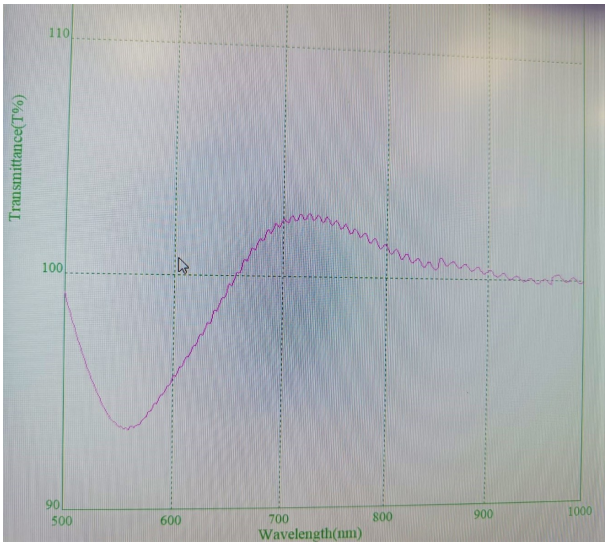

Figure 5.3: Transmittance % corresponding to different wavelengths given by UV-Spectroscopy.

In a particular wavelength interval, we count the number of peaks the graph has and using that we find the thickness of shell using the eq(4.2). We took the following readings,

- $\lambda_1 = 700nm$ and $\lambda_2 = 800nm$
- $n = 12$

Putting the data in eq(4.2) we get the following,

$$d = \frac{12 \cdot 700 \cdot 800 \cdot 10^{-9}}{2 \cdot 100} \, m \tag{5.1}$$

Thus the thickness of the cell was found to be,

$$\boxed{d = 30.8\mu m} \tag{5.2}$$

5.2.2 Pohl Interferometry Technique

We get the following fringes using the Pohl-Interferometer and the cell kept at $\theta = 45°$ from the path of the light beam. Green-colored laser was used for the measurement.

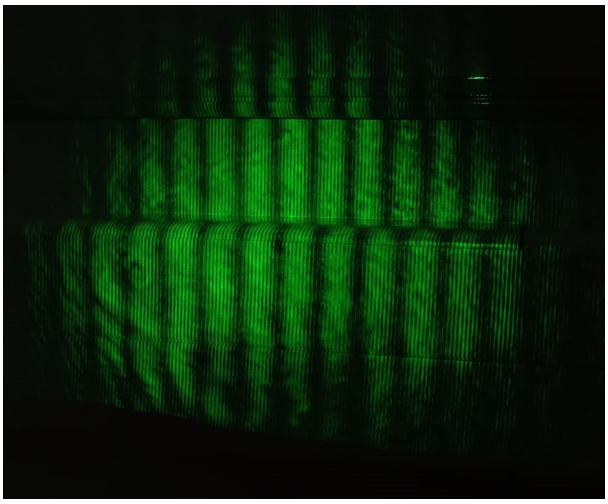

Figure 5.4: Fringes obtained while looking at interference caused by the cell due to its finite thickness by using a Pohl-Interferometer technique. The broader bands corresponds to the thickness of the cell, and the lighter interference pattern bands corresponds to the thickness of individual glass slides used to make the overall cell.

The following table shows the different values noted down for this part. The distance between the screen and the laser setup is $Z = 246.5\ cm$.

S.I. no.	Distance between the fringes (cm)	no. of fringes	Δx
1	6.9	3	2.3
2	9.2	4	2.3
3	10.5	5	2.25
4	18	8	2.12

The average value of Δx was found to be, $\Delta x = 2.28\ cm$, and $\lambda = 532\ nm$ is the wavelength of the laser used. Using the eq(4.1), we get the following value for thickness of the cell,

$$\boxed{d = 40.67\mu m} \tag{5.3}$$

We can clearly see that there's a huge difference between the thickness of the cell obtained using Pohl-Interferometry technique and UV-Spectroscopy method. The errors will be discussed in the next chapter.

5.2.3 Cell used for Fréedericksz Transition Measurements

It's important to point out the fact that the cell for which the above calculations were done, was not used to consider the Fréedericksz Transition. The thickness of the cell was outside the range for which either the B- or K-compensate can be used reliably to get the wavelength measurement. To have uniformity in the data taken by all students, an industrially manufactured cell of cell thickness $d = 5.55\ \mu m$ was used.

5.3 Birefringence Measurement

In this section, we measure the birefringence for our $8CB$ sample using two types of wavelength compensator, i.e., B-compensator and K-compensator. The following is the chart referenced to find the value of θ_1 and θ_2.

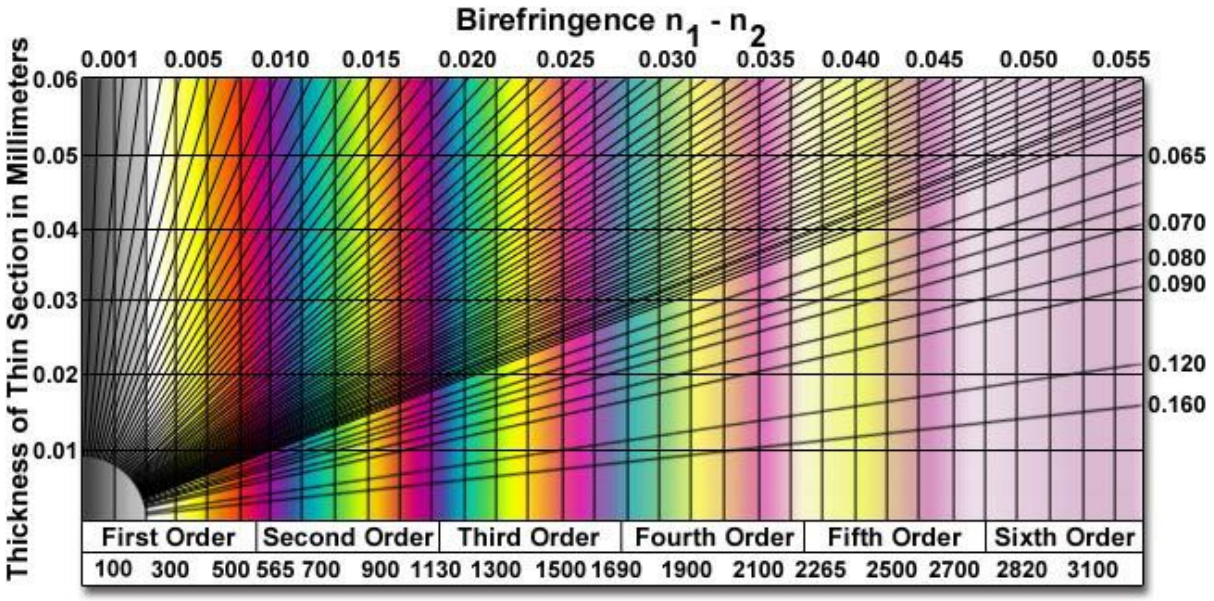

Figure 5.5: Michael-Levy chart that is referenced for birefringence measurements.[11]

5.3.1 Using K-compensator

The working formula for K-compensator is given by,

$$\log \Gamma = \log f(2i) + \log C \tag{5.4}$$

In our measurement, $\log C = 4.841$ as we are using $\lambda = 546\ nm$. Now, we can find Δn from Γ as,

$$\Delta n = \frac{\Gamma}{d} \tag{5.5}$$

where, d is the thickness of the cell used, and γ is found by taking the anit-log of the value of $\log(\Gamma)$ using the anti-log values given in the K-compensator manual. The following is the graph obtained for Δn vs $T(^\circ C)$.

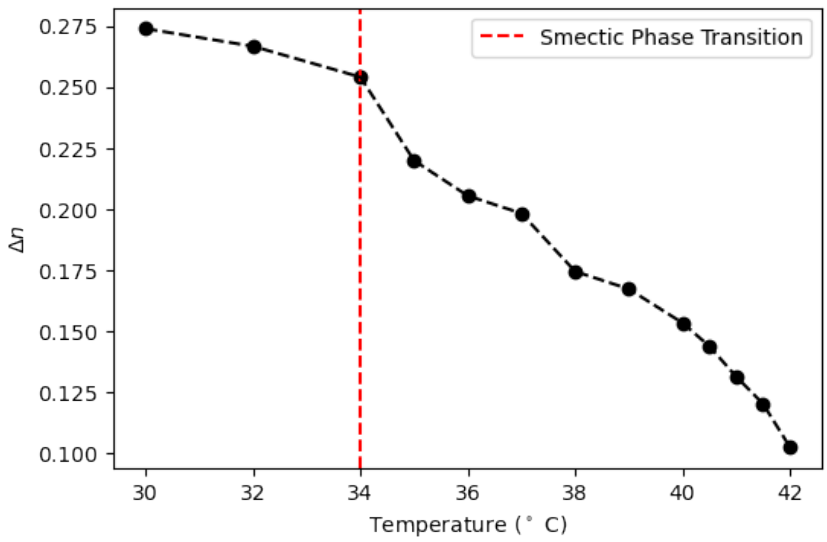

Figure 5.6: Change of Birefringence values with respect to change of temperature while using a K-compensator.

5.3.2 Using B-compensator

The working formula for phase difference is given by,

$$\Gamma_\lambda = d \cdot n_0 \left| \sqrt{1 - \frac{\sin^2 i}{n_e^2}} - \sqrt{1 - \frac{\sin^2 i}{n_0^2}} \right| \tag{5.6}$$

The values such as n_e, and n_o are taken from the B-compensator manual. Birefringence can thus be found as,

$$\Delta n = n_0 \left| \sqrt{1 - \frac{\sin^2 i}{n_e^2}} - \sqrt{1 - \frac{\sin^2 i}{n_0^2}} \right| \tag{5.7}$$

The following graph was obtained between birefringence and temperature.

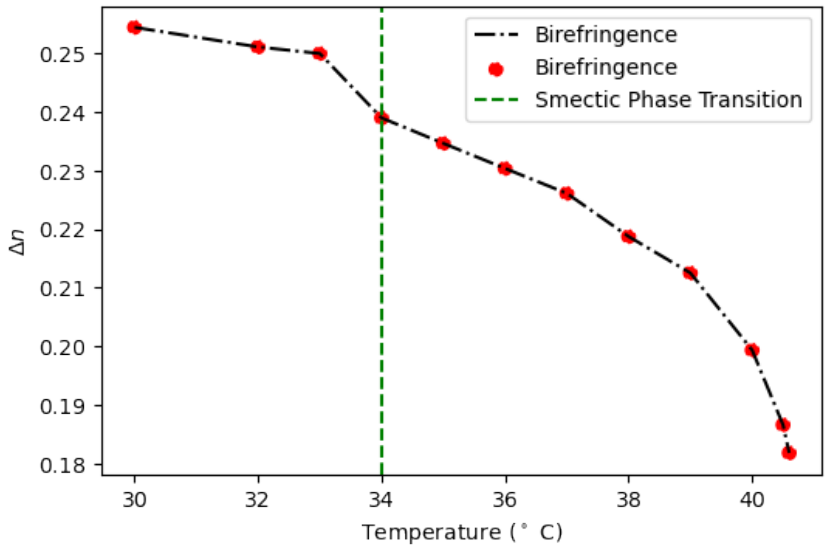

Figure 5.7: Change of Birefringence values with respect to change of temperature while using a B-compensator.

We can see that for K-compensator there's an indication of a secondary phase transition, the occurrence of whose is not explained in this report. To count for this, we checked the same cell using B-compensator which has a better wavelength range. This fixes the error which was coming up in the birefringence values calculated using K-compensator.

5.4 Electric Fréedericksz Transition

In this chapter, we arrive at the main part of the experiment–i.e., Fréedericksz Transition. First, we'll look at the relationship between capacitance (nF) and input voltage (V).

5.4.1 Various Capacitance-related Quantities

We now look at capacitance at low voltage and high voltage limit, namely C_0 and C_∞. Then we will move on to find the related quantities such as $\epsilon_{||}$ and $\epsilon_\perp$, which can be ultimately be used to find the splay and bend elastic constants (k_{11} and k_{33}). Fig(7.3) shows the relationship between capacitance (nF) and input voltage (V) for different temperatures. We can see that the nature of all graphs are same.

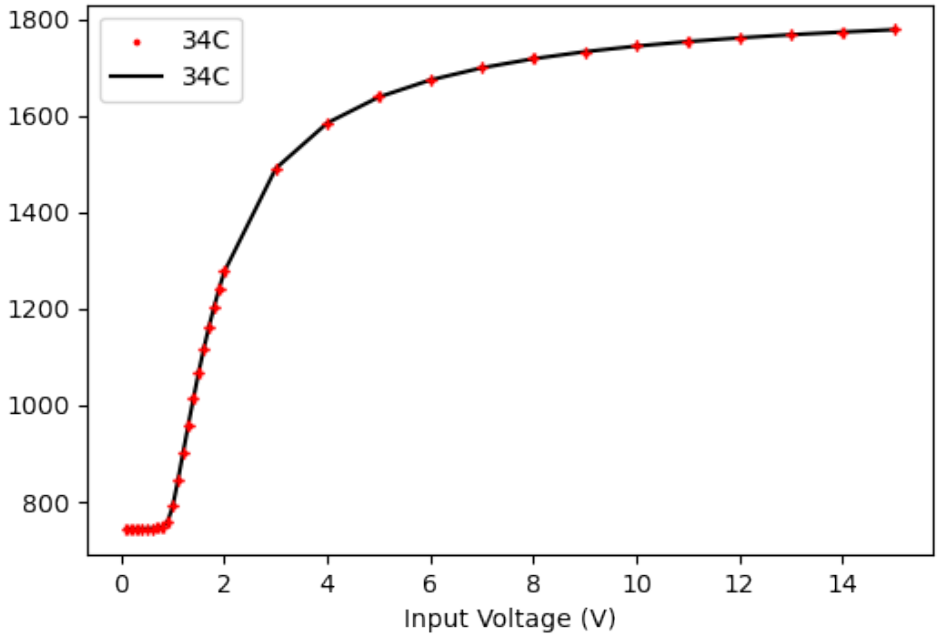

Figure 5.8: Voltage (V) vs Capacitance (nF) for $T = 34°\ C$. The error bars used for the graph are as follows $x_{\text{err}} = 0.1$ V and $y_{\text{err}} = 0.01$ nF.

We need to find low voltage capacitance, we take the capacitance values before what we term as critical voltage (kink in the graph(5.9)). Then we do a linear fit on it, and the intercept of the graph yields low field capacitance value (C_0). The following is one of the graph shows the linear fit for low field capacitance value.

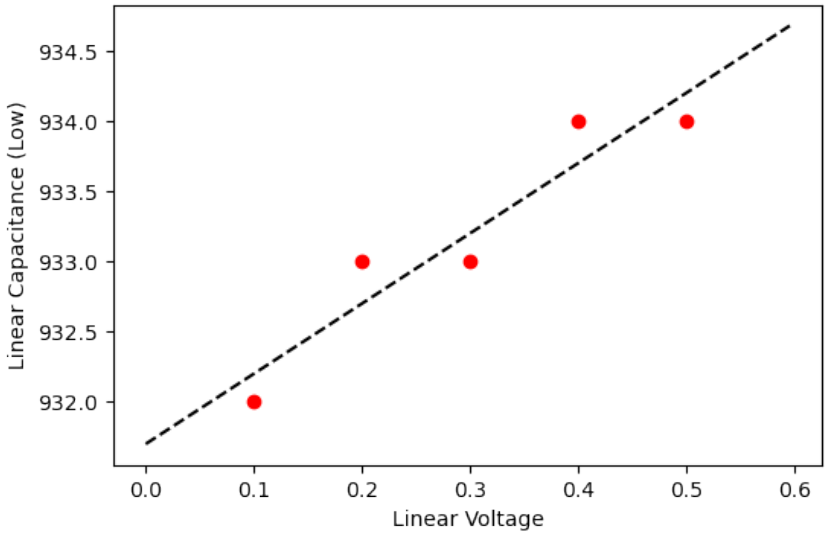

Figure 5.9: Linear curve fit for low field capacitance (C_0) values against the input voltage. Intercept of the above graph gives us C_0 value corresponding to this particular temperature. Same process was done for all temperatures.

Now using the relation between capacitance (C) and $\epsilon_\perp$. To find that we find the graphs for low field capacitance, and high field capacitance. The following are the graphs obtained,

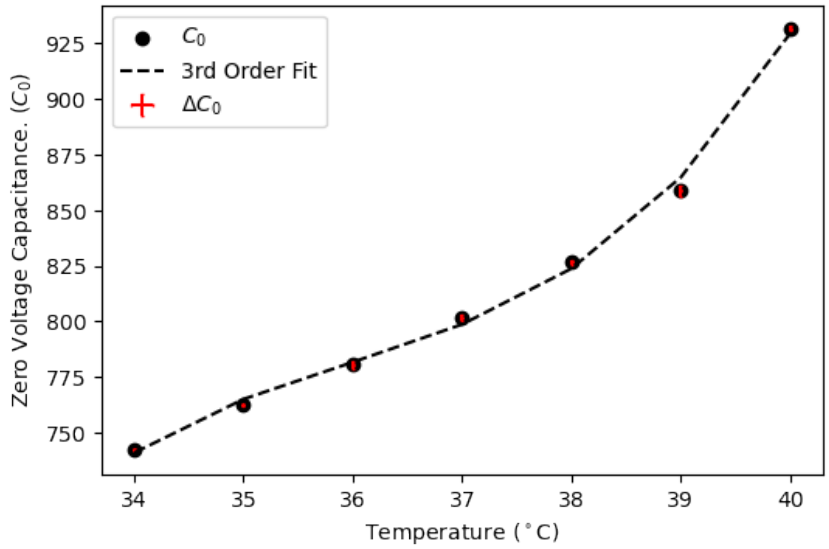

Figure 5.10: Low field Capacitance (pF) vs Voltage (V) denoted by C_0. The low field capacitance value (C_0) shows a 3rd order polynomial fit for different temperatures.

The following is the equation of best fit found for the above curve,

$$\boxed{C_0 = 1.29V^3 - 140.09V^2 + 5053.11V - 60157} \tag{5.8}$$

Now, we move onto finding high-field capacitance values, i.e., the saturation value of capacitance at high input voltages. We do this by taking the value of capacitance after around $2V_c$, plot it with respect to inverse voltage. Now, we do a linear fit on the above two values, and the intercept will give us the high-field capacitance value (C_∞).

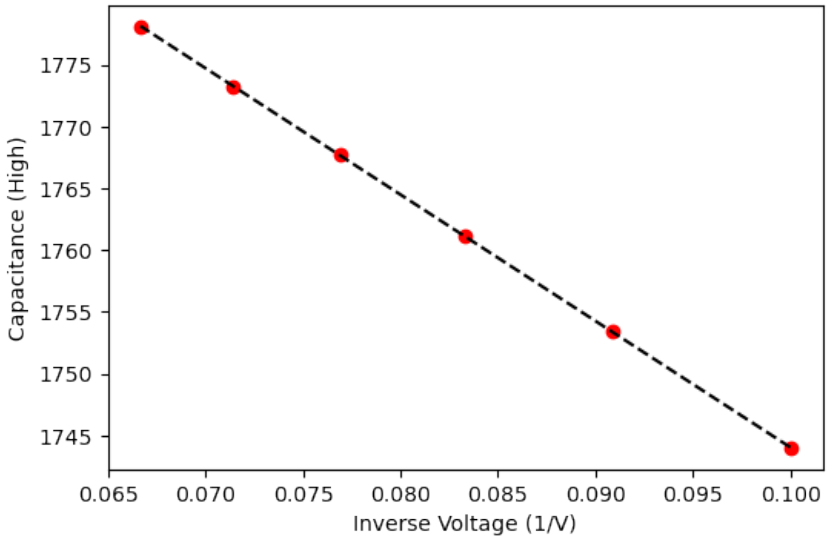

Figure 5.11: Linear curve fit for high field capacitance (C_0) values against the inverse-voltage. Intercept of the above graph gives us C_∞ value corresponding to this particular temperature. Same process was done for all temperatures.

The graph between high-field capacitance and input voltage is found to be,

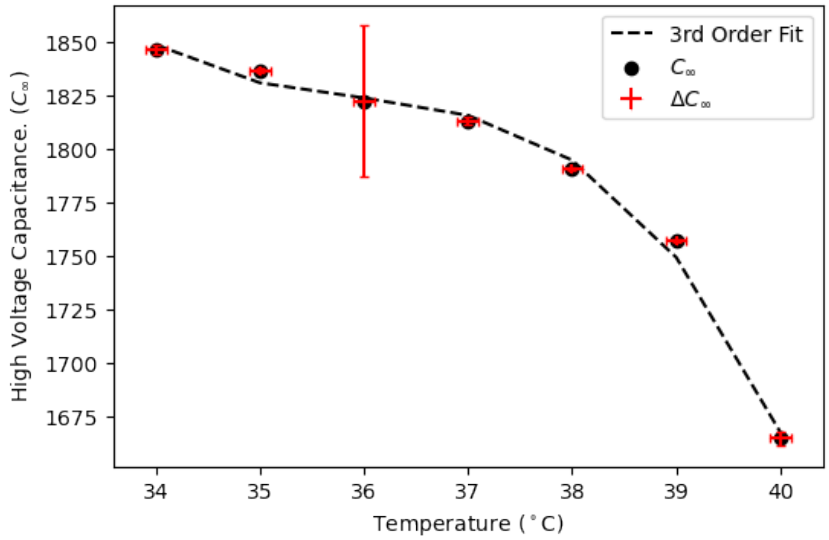

Figure 5.12: High field Capacitance (pF) vs Voltage (V) denoted by C_∞. The high field capacitance value (C_∞) shows a 3rd order polynomial fit for different temperatures.

The following is the curve fit equation for C_∞ from the above graph,

$$\boxed{C_\infty = -1.95V^3 + 210.43V^2 - 7562.01V + 92724} \tag{5.9}$$

The value of error-bars will be mentioned in the next chapter along with error-analysis of all other quantities. Before doing so we need to find the critical voltage value for each temperature. We find the value of $\epsilon_{||}$ and $\epsilon_\perp$ using the values of C_0 using the relationship mentioned in eq(2.8). The following is the graph obtained for $\epsilon_{||}$ and $\epsilon_\perp$ for different temperature measurements.

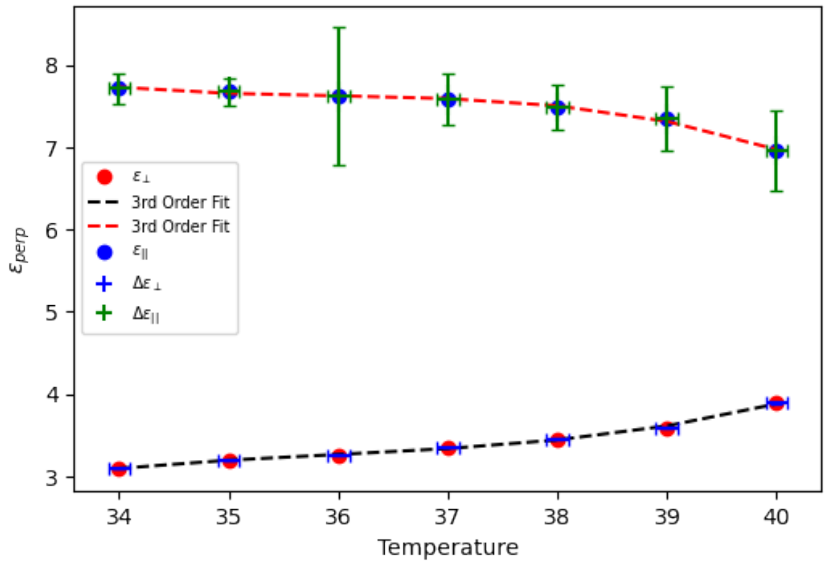

Figure 5.13: Change in $\epsilon_{||}$ and $\epsilon_\perp$ for different temperatures. The error bars are discussed in next chapter.

Using the values of $\epsilon_{||}$ and $\epsilon_\perp$, we can calculate the reduced permittivity (γ) as dictated by eq(2.3). The following graph was obtained for γ for different values of temperature.

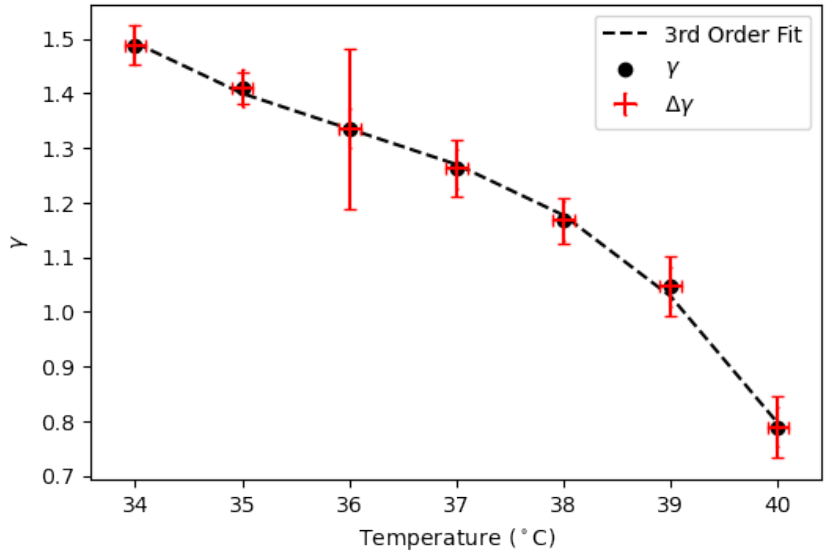

Figure 5.14: Reduced permittivity (γ) for different temperatures. The error bars are discussed in next chapter.

The following is the equation of 3rd order linear fit.

$$\boxed{\gamma = -0.004T^3 + 0.501T^2 - 18.078T + 219.699} \tag{5.10}$$

5.5 Finding Elastic Constants (k_{11}) and (k_{33})

We'll start by finding the critical voltage values for different temperature measurement. The following graph was obtained,

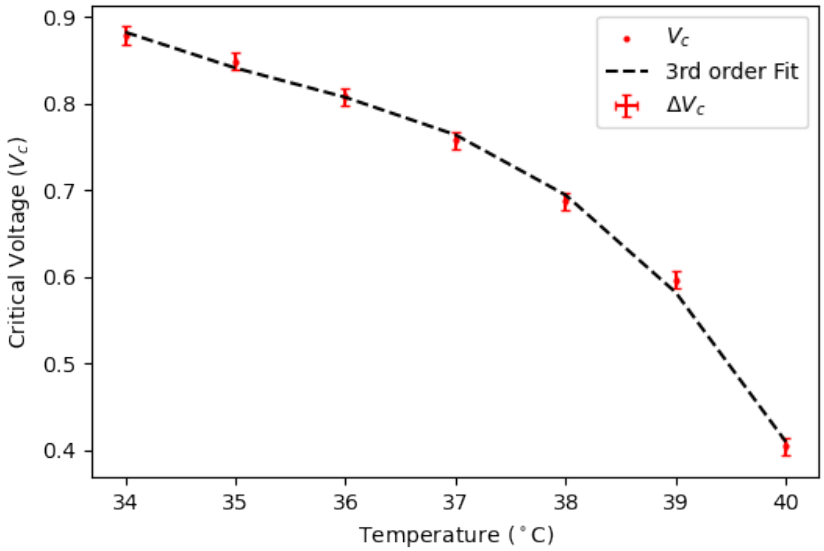

Figure 5.15: Critical voltage values (V_c) for different temperature values. The error bars are discussed in next chapter.

Now, we'll find the value of splay elastic constant (k_{11}) using the eq(2.5). The following is the graph obtained between k_{11} for different temperatures.

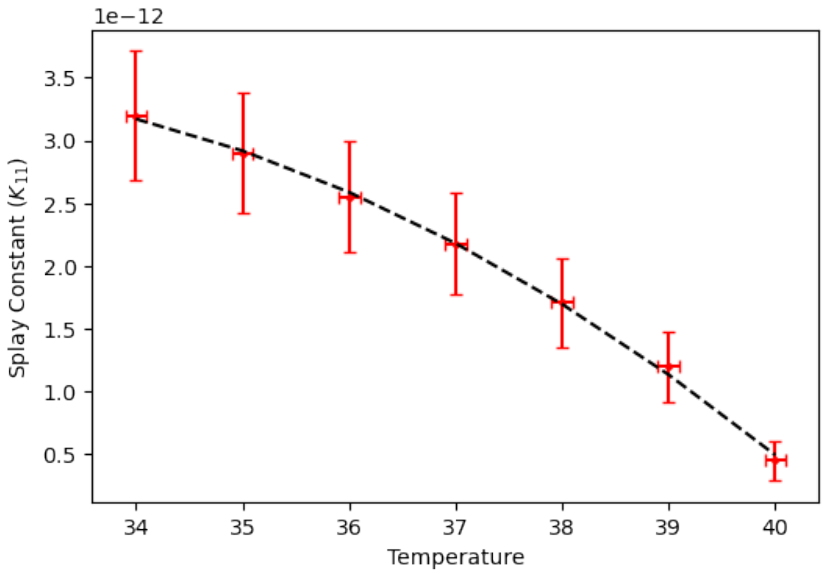

Figure 5.16: Splay Elastic Constant (k_{11}) for different temperature values calculated using critical voltage values (V_c). The error bars are discussed in next chapter.

Now that we've found one splay elastic constant, we need to find the bend elastic constant using κ values. One problem is that the calculation of κ is very difficult. We consider the low field κ values only for this analysis. To find this, we fit the part of the curve below critical value with a linear fit, and we find the slope of the fit. Now, using the slope value and corresponding fixed value of γ for that temperature using the eq(2.4). The following is the variation of κ with temperature.

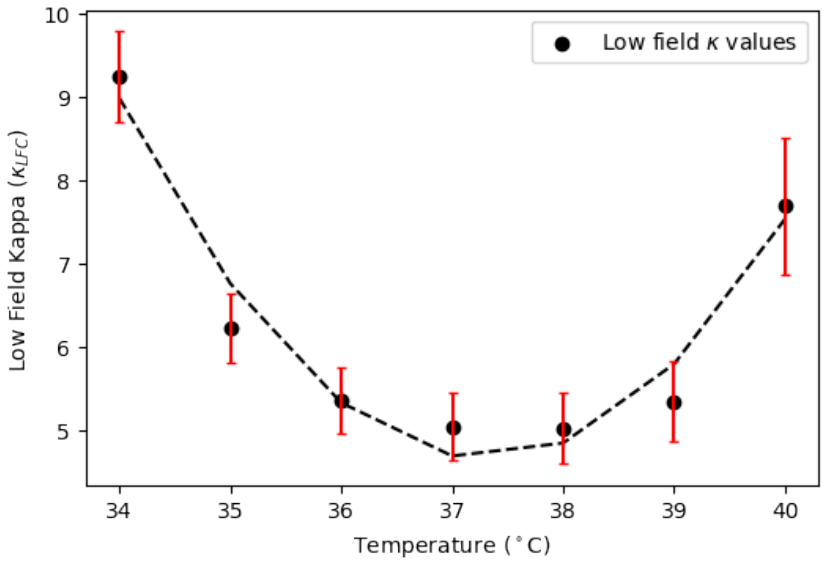

Figure 5.17: κ_{LFC} for different temperature values calculated using critical voltage values (V_c). The error bars are discussed in next chapter.

The equation for best fit second order curve is as follows,

$$\boxed{\kappa_{\text{LFC}} = 0.39T^2 - 29.59T + 556.49} \tag{5.11}$$

Now that we've k_{11} and κ_{LFC} for different temperature values, we can find the value of k_{33} using eq(**??**). The graph obtained for k_{33} for varying temperature is shown below,

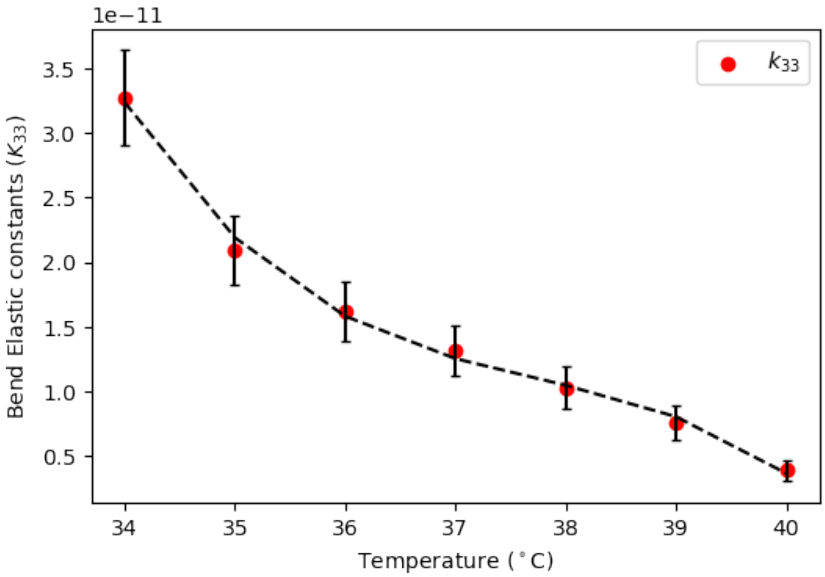

Figure 5.18: k_{33} for different temperature values calculated using critical voltage values (V_c). The error bars are discussed in next chapter.

The above data was fitted with a 3$^{\text{rd}}$ order polynomial fit. The equation for the curve fit is found to be,

$$\boxed{k_{33} = -(2.64 \cdot 10^{-13}) \times T^3 + (0.03 \cdot 10^{-13}) \times T^2 - (0.01 \cdot 10^{-11}) \times T + (1.43 \cdot 10^{-8})} \tag{5.12}$$

Just to compare the trend of both the elastic constants with temperature, we plot them on the same area and we get the graph below.

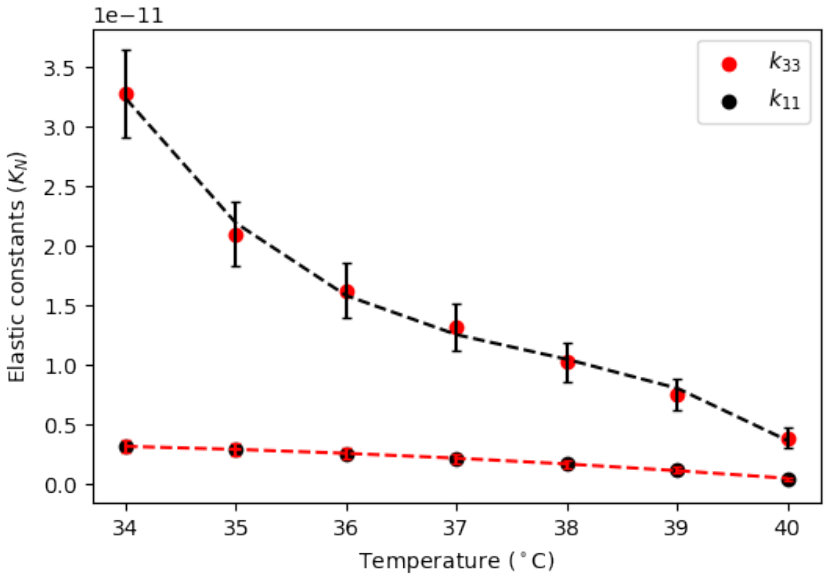

Figure 5.19: k_{33} and k_{11} for different values of temperatures plotted on the same graph. The error bars are discussed in next chapter.

Chapter 6

Error Analysis

One of the most important aspect of experimental study is the error analysis associated with the measurements done. In this chapter, we'll go step by step into various formulae that was used to calculate the final outcome and we'll calculate the error propagated due to each step. Here are the "milestones formulae" which contributes the most towards the final data measurement.

6.1 Error in γ

We know the relationship between γ, C_∞, and C_0. Thus, we can find the error in γ as,

$$d\gamma = \pm\gamma\sqrt{\left(\frac{dC_\infty}{C_\infty}\right)^2 + \left(\frac{dC_0}{C_0}\right)^2} \tag{6.1}$$

The following is the table containing the values of error in γ values using the above eq(6.1).

$C_0\ (nF)$	$C_\infty\ (nF)$	γ	$\Delta\gamma$
0.74	1.85	1.49	$\pm$0.04
0.76	1.84	1.41	$\pm$0.03
0.78	1.82	1.34	$\pm$0.15
0.80	1.81	1.26	$\pm$0.05
0.82	1.79	1.16	$\pm$0.04
0.85	1.76	1.04	$\pm$0.05
0.93	1.66	0.79	$\pm$0.06

6.2 Error in $\epsilon_\perp$

The error in the value for the perpendicular dielectric constant can be calculated as,

$$\epsilon_\perp = \frac{LC_0}{A} \tag{6.2}$$

Now, L and A are given industrial value and hence we consider $dL = dA = 0$ as it wasn't provided with the cell to us.Therefore, the error in $\epsilon_\perp$ can be written as,

$$d\epsilon_\perp = \pm\frac{dC_0}{C_0}\cdot\epsilon_\perp \tag{6.3}$$

The following table consists of all the errors associated with $\epsilon_\perp$.

$C_0\ (nF)$	$\epsilon_\perp$	$\Delta\epsilon_\perp$
0.74	3.102	$\pm$0.001
0.76	3.196	$\pm$0.001
0.78	3.262	$\pm$0.007
0.80	3.351	$\pm$0.006
0.82	3.465	$\pm$0.004
0.85	3.599	$\pm$0.010
0.93	3.890	$\pm$0.004

6.3 Error in $\epsilon_{||}$

Now, we know a relationship between $\epsilon_\perp$, γ, and $\epsilon_{||}$ as,

$$\frac{d\epsilon_{||}}{\epsilon_{||}} = \sqrt{\left(\frac{d\gamma}{\gamma}\right)^2 + \left(\frac{d\epsilon_\perp}{\epsilon_\perp}\right)^2} \tag{6.4}$$

The following table contains the value of $\Delta\epsilon_{||}$ obtained using the above equaiton.

γ	$\epsilon_{||}$	$\Delta\epsilon_{||}$
1.49	7.72	$\pm$0.19
4.41	7.68	$\pm$0.16
1.34	7.62	$\pm$0.83
1.26	7.58	$\pm$0.31
1.16	7.49	$\pm$0.26
1.04	7.35	$\pm$0.39
0.79	6.96	$\pm$0.49

6.4 Error in k_{11}

Now, we'll look at the error propagation for the splay elastic constant measurement value, i.e., k_{11}. We used the following formula for calculation of k_{11},

$$k_{11} = \left(\frac{v_c}{\pi}\right)^2 (\epsilon_0 \epsilon_\perp \gamma) \tag{6.5}$$

Therefore, from the quadrature formula the error propagated in k_{11} (the equation below is for relative error) can be written as,

$$\left(\frac{dk_{11}}{k_{11}}\right) = \sqrt{2\left(\frac{dV_c}{V_c}\right)^2 + \left(\frac{d\epsilon_\perp}{\epsilon_\perp}\right)^2 + \left(\frac{d\gamma}{\gamma}\right)^2} \tag{6.6}$$

The following is the table containing all the errors associated with the measurement of k_{11}.

γ	$\epsilon_\perp$	V_c(V)	$k_{11}(\times 10^{-12})$(N/m^2)	$\Delta k_{11}(\times 10^{-12})$(N/$m^2$)
1.49	3.102	0.878	3.196	0.514
4.41	3.196	0.848	2.900	0.483
1.34	3.262	0.808	2.551	0.446
1.26	3.351	0.758	2.177	0.406
1.16	3.465	0.686	1.705	0.351
1.04	3.599	0.596	1.196	0.283
0.79	3.890	0.404	4.493	0.157

6.5 Error in κ

To find k_{33}, we need the quantity κ which relates k_{11} and k_{33}. κ depends on γ and the slope of the linear fit for low field voltages ($v/v_c = 1$). The error in κ can be written as,

$$d\kappa = \kappa\sqrt{\left(\frac{d\gamma}{\gamma}\right)^2 + \left(\frac{dm}{m}\right)^2} \tag{6.7}$$

The following is the error values calculated for κ using various values.

γ	Δm	κ	$\Delta\kappa$
1.49	2.06	9.23	± 0.08
4.41	1.04	6.22	± 0.03
1.34	35.23	5.36	± 0.10
1.26	1.50	5.04	± 0.04
1.16	0.88	5.02	± 0.03
1.04	0.56	5.34	± 0.19
0.79	2.06	7.68	± 0.12

6.6 Error in k_{33}

The error in k_{33} can be found using the relationship between k_{11} and κ as,

$$dk_{33} = k_{33}\sqrt{\left(\frac{dk_{11}}{k_{11}}\right)^2 + \left(\frac{d\kappa}{\kappa}\right)^2} \tag{6.8}$$

The following consists the errors found for k_{33} associated with experimental measurements.

κ	$\Delta\kappa$	$\Delta k_{11}(\times 10^{-13})$(N/$m^2$)	$k_{33}(\times 10^{-12})$(N/m^2)	$\Delta k_{33}(\times 10^{-12})$ (N/m^2)
9.23	± 0.08	5.144	32.714	5.272
6.22	± 0.03	4.833	20.937	3.491
5.36	± 0.10	4.464	16.218	4.182
5.04	± 0.04	4.063	13.142	2.456
5.02	± 0.03	3.511	10.262	2.113
5.34	± 0.19	2.839	7.580	1.799
7.68	± 0.12	1.572	3.901	1.367

Chapter 7

Conclusion and Discussions

7.1 Conclusion

In this experimental study, we worked with $8CB$ Liquid Crystal compound and tried to study the optical property known as "birefringence". Moreover, the study involved studying the Fréedericksz transition and calculate the splay and bend elastic constant, i.e., k_{11} and k_{33} respectively. This was done through the low and high field capacitance value calculated for all of the temperature values (i.e., $34 - 40°$C). Moreover, the perpendicular ($\epsilon_{\perp}$) and the parallel ($\epsilon_{||}$) permittivity was calculated which was then used to find the value of reduced permittivity (γ). Lastly, all of this was used to find the the splay elastic constant (k_{11}). Now, at low values of voltages (below the critical voltages) the value of κ was calculated which was used to find the value of bend elastic constant (k_{33}). The overall nature of all the graphs obtained were similar to that obtained in (Morris 1986) which also uses the 8CB liquid crystal compound. The optical Fréedericksz transition was not explored in this report as the data analysis was too complicated to be conducted at the current level. However, basic analysis was done and the graph between phase difference (d_0) and temperature (T) was obtained which is included in the repository mentioned in appendix.

7.2 Discussions

There are various sources of errors associated with the experimental measurements. The preparation of the cells were not done in a clean room which can add some experimental errors, but as the cells prepared by us was not used in the Fréedericksz Transition study, this error can be ignored from the final error analysis. However, the way cell is prepared can effect the final data in an extreme manner. The edge effects of the cell will be more prominent if the edges of the cell are asymmetric or uneven due to improper placement of one slide over the other to make the chamber. One important source of error is in the measurement of the bend elastic constant (k_{33}) as it requires us to extrapolate the value of κ from the graph between reduced voltage (v) and reduced capacitance (c). There were three ways in which κ can be extrapolated as mentioned in (Morris 1986). First, being extrapolating the value of κ at low field values, i.e., linear fit between v and c at voltages below the critical voltage (v_c). However, one problem with this approach is deciding the limit of critical voltage (v_c), i.e., the point of transition. Due to discrepancy in deciding this value, the overall calculation of κ_{LFC} which can lead to erroneous results in calculation of k_{33}. Another approach could've been extrapolating the value of κ at high field values. However, this approach requires the use of an integrator, and the overall steps were not clearly defined in (Morris 1986) which was followed throughout the data analysis. Last method was to extract κ by doing a complete non-linear fit for each of the γ values. The best fit curve was determined by I to be a 3rd order polynomial for a section of the graph, however there were 4 coefficients associated with the 3^{rd} order fit, and there was no clear indication to which could've been the required values of κ_{HFC}. Due to limited information about the latter two methods, low field κ was calculated and was used to find the value of bend elastic constant (k_{33}). Proper error calculations has been done for all of the values, and has been presented in the previous chapter. However, one point we need to look was the third temperature point (i.e., $T = 36°\ C$). We see a huge error-bar for each of the graphs at this temperature value. All the data calculation was checked several times, and the errors persists. No possible reason for this error-bar jump was identified through this analysis. (Morris 1986) was used to do the complete data analysis and theory concerning this experiment study involving 8CB liquid crystals.

Bibliography

[1] Introduction to liquid crystals - university of Houston. (n.d.). Retrieved February 27, 2023, from https://uh.edu/~chembi/liquidcrystals.pdf

[2] Kumar, Pramoda. "Field Driven Reorientatioal and convective instabilities in Nematic Liquid Crystals," 2010.

[3] D. Schmidt, M. Schadt, W. Helfrich, Z. Naturforsch A. 27, 277 (1972).

[4] K. V. Le, F. Araoka, K. Fodor-Csorba, K. Ishikawa, H. Takezoe, Liq. Cryst. 36,1119 (2009).

[5] L. Kovalenko, M. W. Schroder, R. A. Reddy, S. Diele, G. Pelzl, and W. Weissflog, Liq. Cryst. 32, 857 (2005).

[6] O. D. Lavrentovich, V. G. Nazarenko, V. V. Sergan, and G. Durand, Phys. Rev. A 45, R6969 (1992).

[7] S. W. Morris. "*Measurement of the Elastic Constant of Liquid Crystals*," 1981.

[8] Birefringence, WikiPedia. Accessed 13.04.2023. https://en.wikipedia.org/wiki/Birefringence

[9] Research Gate. Rubbing Machine. Accessed May 05, 2023. LINK

[10] UV-vis spectroscopy: Principle, strengths and limitations and applications. Analysis & amp; Separations from Technology Networks. (2021, June 30). website

[11] Michel-Levy Birefringence chart. Specialized Microscopy Techniques - Michel-Levy Birefringence Chart — Olympus LS. (n.d.). Retrieved May 6, 2023, from https://www.olympus-lifescience.com/en/microscope-resource/primer/techniques/polarized/michel/

Acknowledgement

This experiment was done towards the completion of the course, "Physics Lab V" offered by Dr Pramoda Kumar. First, I would like to thank the Professor for offering this wonderful course, and and helping us learn various experimental techniques. I would further like to thank the teaching fellow Ankit Gupta for helping extensively throughout the semester and making various parts of the laboratory more accessible for us. I would also like to thank my class mates– Kushal, Shwetha, and Vineet for all fun-learning time throughout the semester.

Appendix

7.3 Extra Graphs

Please find the extra details from experimental analysis in this sections. Here are the graphs between capacitance and voltage for various temperatures.

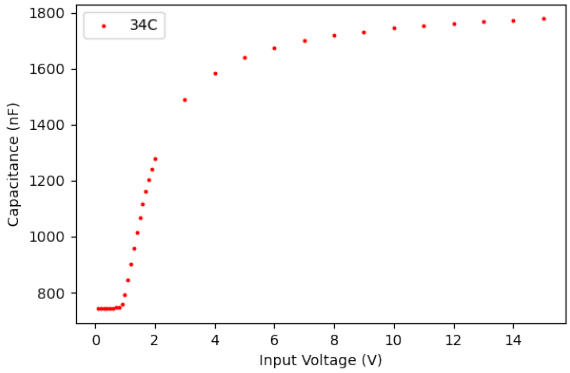

(a) Voltage (V) vs Capacitance (nF) for Temperature $= 34^{\circ}\ C$.

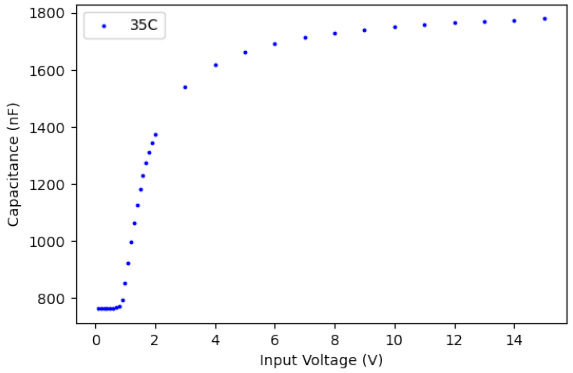

(b) Voltage (V) vs Capacitance (nF) for Temperature $= 35^{\circ}\ C$.

Figure 7.1: Voltage vs Capacitance for different temperature values.

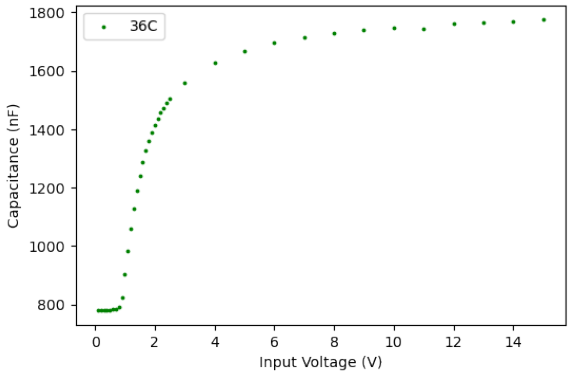

(a) Voltage (V) vs Capacitance (nF) for Temperature $= 36^{\circ}\ C$.

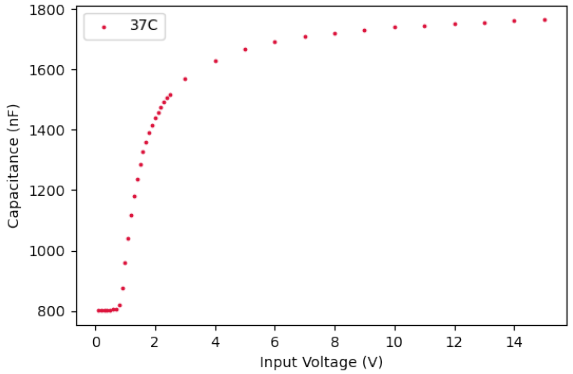

(b) Voltage (V) vs Capacitance (nF) for Temperature $= 37^{\circ}\ C$.

Figure 7.2: Voltage vs Capacitance for different temperature values.

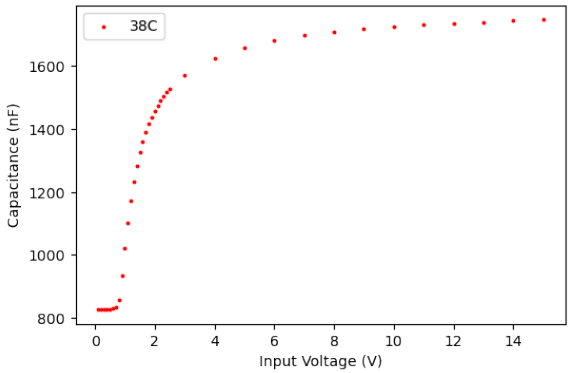

(a) Voltage (V) vs Capacitance (nF) for Temperature $= 38^{\circ}\ C$.

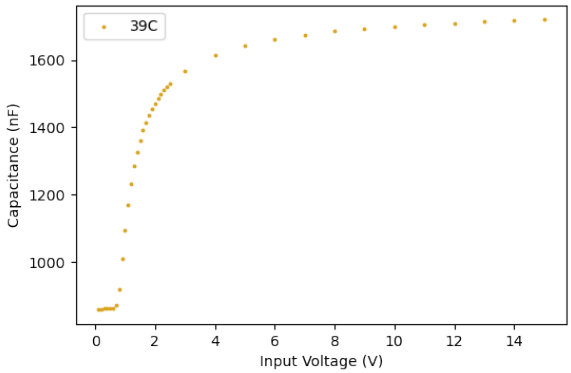

(b) Voltage (V) vs Capacitance (nF) for Temperature $= 39^{\circ}\ C$.

Figure 7.3: Voltage vs Capacitance for different temperature values.

7.4 Analysed Data

Find the attached link to the github repository which contains the data files, and the python code file which was used for data analysis, interfacing, and error analysis:
https://github.com/ninjha252/Nematic-Liquid-Crystals.git